Synthesis and Properties of Soy Hull-Reinforced Biocomposites from Conjugated Soybean Oil

Rafael L. Quirino, Richard C. Larock

Department of Chemistry, Iowa State University, Ames, Iowa 50011

Received 12 August 2008; accepted 14 December 2008
DOI 10.1002/app.29660
Published online 12 February 2009 in Wiley InterScience (www.interscience.wiley.com).

ABSTRACT: The tensile and flexural properties of new thermosetting composites made by the free radical polymerization of a conjugated soybean oil (CSO)-based resin reinforced with soy hulls have been determined for various resin compositions. The effects of reinforcement particle size and filler/resin ratio have been assessed. The thermal stability of the new materials has been determined by thermogravimetric analysis and the wt % of oil incorporation has been calculated after Soxhlet extraction (the extracts have been identified by ^{1}H-NMR spectroscopy). The resin consists initially of 50 wt % CSO and varying amounts of divinylbenzene (DVB; 5–15 wt %), dicyclopentadiene (DCPD; 0–10 wt %), and *n*-butyl methacrylate (BMA; 25–35 wt %). Two soy hull particle sizes have been tested (<177 and <425 μm) and two different filler/resin ratios have been compared (50 : 50 and 60 : 40). An appropriate cure sequence has been established by differential scanning calorimetry (DSC) analysis. The results show a decrease in the properties whenever DVB or BMA is substituted by DCPD. Also, larger particle sizes and higher filler/resin ratios are found to have a negative effect on the tensile properties of the new materials. © 2009 Wiley Periodicals, Inc. J Appl Polym Sci 112: 2033–2043, 2009

Key words: biodegradable; biomaterials; biopolymers; composites

INTRODUCTION

The replacement of petroleum-based products by materials prepared from natural biorenewable resources has been intensively investigated in recent years in an attempt to reduce man's dependence on crude oil. One promising approach involves the use of vegetable oils in substitution or in addition to petroleum derivatives. Interesting applications as biofuels,[1] coatings,[2] and biomaterials[3] (biopolymers and biocomposites) have been reported.

The use of vegetable oils as comonomers in the synthesis of new biopolymers is known and a variety of processes and materials have already been reported in the literature using different vegetable oils.[4–6] A simple and promising procedure that yields thermosets with unique mechanical properties involves the reaction of the carbon–carbon double bonds in the fatty acid chains of triglycerides with other reactive monomers [divinylbenzene (DVB), styrene, acrylonitrile, dienes, acrylates, etc.] to form a network of crosslinked polymer chains. These materials can be obtained through cationic,[7–10] thermal,[11,12] or free radical polymerization.[13,14] Initially, our group focused on the development of new resins using a range of vegetable oils, including soybean,[7,10,14] corn,[8] tung,[11] and linseed[12,13] oils.

Soybeans are among America's largest crops, being mainly used in the food industry. Soybean oil represents a readily available and low-cost starting material that can be used for the purposes indicated earlier.[1–3] The fatty acid composition of soybean oil is as follows: 51% linoleic acid (C18:2), 23% oleic acid (C18:1), 10% palmitic acid (C16:0), 7% linolenic acid (C18:3), 4% stearic acid (C18:0), and 5% of other fatty acids in negligible amounts.[15]

With an average of 4.5 double bonds per triglyceride,[10] soybean oil is only moderately active toward free radical species, but the reactivity can be considerably increased by the conjugation of the carbon–carbon double bonds of the fatty acid chains. Several studies regarding the double-bond isomerization of vegetable oils have been reported in the literature.[16–19] Our group has developed a homogeneous isomerization procedure employing $[RhCl(C_8H_{14})_2]_2$ as a precatalyst.[20] The reaction yields >95% conjugation for several vegetable oils tested and has been frequently used in our work on bioplastics.[7,13,21–24]

Free radical resins developed in our group so far include conjugated linseed oil-[13] and conjugated soybean oil (CSO)[14]-containing biopolymers. The results obtained in these studies revealed that a vegetable oil content ranging from 40 to 65 wt % maximizes

Correspondence to: R. C. Larock (larock@iastate.edu).

Contract grant sponsors: Iowa Biotechnology Consortium (through the USDA), Recycling and Reuse Technology Transfer Center of the University of Northern Iowa.

the oil incorporation in the final matrix.[14] More recently, in an attempt to obtain stronger materials, we have reported the preparation and properties of composites containing a tung oil-based resin (cured by free radical polymerization) reinforced with spent germ, an underused agricultural byproduct from wet-mill ethanol production.[25]

Soy hulls, another example of an abundant underused agricultural byproduct, are essentially the outer skin of the soybean.[26] They are normally used as a low-cost feedstock or discarded during processing of the soybeans. The large quantity of soy hulls produced and their lack of industrial application account for their low price.[27] The chemical composition of soy hulls is approximately 11% protein, 11% galactomannans, 12% acidic polysaccharides, 10% xylan hemicelluose, 40% cellulose, and 16% lignin.[27] Because of their relatively high fiber content (lignin, cellulose, and hemicellulose), low cost, and ready availability, soy hulls are particularly attractive as an economical and environmentally friendly reinforcement for biocomposites.

In this work, we have studied the mechanical and flexural properties of composites prepared from CSO reinforced with soy hulls. An appropriate cure sequence has been established by means of differential scanning calorimetry (DSC). Young's (E) and storage (E') moduli, as well as tensile strengths and glass transition temperatures (T_gs) have been determined as the resin composition is varied. We have also looked into the effect of the particle size and the filler/resin ratio on the properties of the final materials. Their thermal stability has been assessed by thermogravimetric analysis (TGA), the wt % incorporation of CSO in the resin has been determined by Soxhlet extraction with CH_2Cl_2, and the extracts have been identified by ^{1}H-NMR spectroscopy. A scanning electron microscopy (SEM) study has shown visual proof of the filler–resin arrangements in the final composites.

EXPERIMENTAL

Materials

n-Butyl methacrylate (BMA) and dicyclopentadiene (DCPD) were purchased from Alfa Aesar (Ward Hill, MA). DVB and *t*-butyl peroxide (TBPO) were purchased from Aldrich Chemical (Milwaukee, WI). All chemicals were used as received. The soybean oil (*Carlini* brand; Aldi, Batavia, IL) was purchased in a local grocery store, and conjugation was carried out using a homogeneous Rh catalyst, as described in the literature,[20] to produce CSO. The soy hulls were provided by West Central (Ralston, IA). They were ground and sieved into two different particle sizes, <425 μm diameter (>40 mesh) and <177 μm diameter (>80 mesh). The sieved soy hulls were then dried overnight at 70°C in a vacuum oven before use.

Preparation of the composites

The crude resin was obtained by mixing the designated amounts of each component (CSO, DVB, DCPD, and BMA) in a beaker. All resins have been prepared using 50 wt % CSO. For the radical initiator TBPO, 5 wt % of the total resin was added. As an example of the nomenclature adopted in this work, the sample DVB10-DCPD5-BMA35 represents a resin containing 10 wt % of DVB, 5 wt % of DCPD, and 35 wt % of BMA (the other 50 wt % of the resin being CSO). The dried soy hulls were impregnated with the resin (in the ratios designated in the text) and compression-molded at 276 psi (unless otherwise specified). The filler content could not be reduced below 50 wt %, because, during compression molding, the excess of resin leaks when pressure is applied. If cure occurs at atmospheric pressure, then the fillers accumulate on the bottom of the mold and a nonuniform composite is obtained. For filler compositions above 60 wt %, the opposite effect is observed. The amount of resin was insufficient to completely wet the soy hulls yielding materials that tended to crumble when handled. All composites were cured for 5 h at 130°C and then postcured at 150°C for another 2 h.

Characterization

The optimal cure sequence was determined by DSC using a Q20 DSC (TA Instruments, New Castle, DE) under a N_2 atmosphere over a temperature range of −20 to 400°C at a rate of 20°C/min. The samples weighed ~ 11 mg.

The tensile test experiments were conducted at 25°C according to ASTM D-638 using an Instron universal testing machine (model 5569) equipped with a video extensometer and operating at a crosshead speed of 2.0 mm/min. The dogbone-shaped test specimens had the following gauge dimensions: 57 mm × 12.7 mm × 4.5 mm (length, width, and thickness, respectively).

The dynamic mechanical analysis (DMA) was conducted on a TA Instruments Q800 DMA using a three-point bending mode. A rectangular specimen of about 22 mm × 8.5 mm × 1.5 mm (length × width × thickness) was cut from the samples. Each specimen was cooled to −60°C and then heated at 3°C/min to 250°C at a frequency of 1 Hz under air.

A Q50 TGA instrument (TA Instruments) was used to measure the weight loss of the samples under an air atmosphere. The samples were heated

from room temperature to 650°C at a heating rate of 20°C/min. The samples weighed ~ 10 mg.

Soxhlet extraction was conducted to determine the amount of soluble materials in the composites. A 2 g sample was extracted for 24 h with 110 mL of dichloromethane (CH_2Cl_2). After extraction, the resulting solution was concentrated on a rotary evaporator, and then both the soluble and insoluble materials were dried in a vacuum oven at 70°C overnight before weighing. The soluble fraction of each extracted sample was dissolved in $CDCl_3$ and proton nuclear magnetic resonance (^{1}H-NMR) spectroscopic analysis was carried out to determine its composition. The ^{1}H-NMR spectra were obtained with a Varian Unity spectrometer (Varian Associates, Palo Alto, CA) operating at 300 MHz.

SEM analysis was conducted using a Hitachi S-2460N variable pressure SEM. The parameters used are as follows: 20 kV accelerating voltage, 60 Pa Helium atmosphere, and 15 mm working distance. The equipment was set with a tetra backscattered electron detector. Each sample analyzed was frozen with liquid N_2 prior to fracture for the cryofractured analysis. For comparative reasons, the samples were also cut using a razor blade and analyzed by SEM.

RESULTS AND DISCUSSION

Cure sequence determination

A preliminary determination of the best cure sequence was conducted by means of DSC experiments with a partially cured composite sample [Fig. 1(A)] and with soy hulls alone [Fig. 1(B)]. In Figure 1(A), the DSC curve of the sample DVB15-BMA35 with 50 wt % soy hulls and a particle size <425 μm diameter heated at 130°C for 4 h shows two exothermic peaks at ~ 135 and 170°C, as well as a pronounced absorption of heat at 220°C and two exothermic peaks at 260 and 350°C. Any transitions occuring after 400°C are related to decomposition of the resin as explained in our previous work.[25] The heat flow observed between 200 and 400°C corresponds to decomposition of the hemicellulose and cellulose present in significant amounts in the soy hulls.[28] This same feature can be seen in Figure 1(B). The exothermic peaks at 135 and 170°C in Figure 1(A) are probably related to further cure of the resin.

A comparison of Figure 1(A,B) confirms that the heat flow observed in the range 200–400°C in Figure 1(A) is related to changes in the soy hulls. The lower degradation temperature for the soy hulls alone (the heat absorption starts at 160°C) when compared with the composite analysis [Fig. 1(A), the heat absorption starts at 198°C] suggests that the resin helps to thermally stabilize the filler, increasing considerably the degradation temperatures.

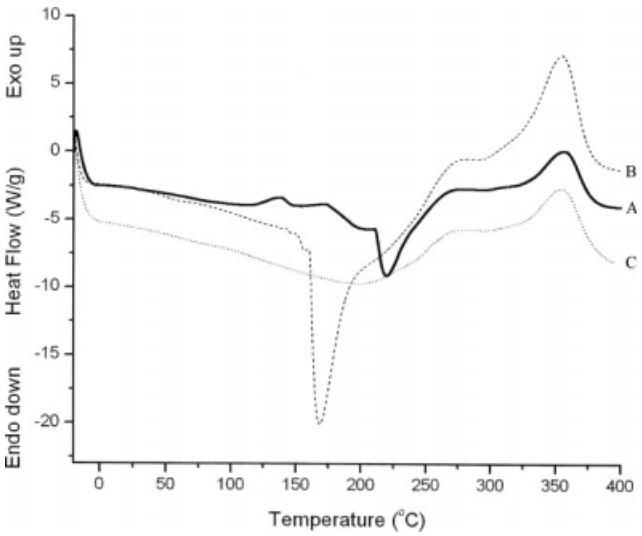

Figure 1 DSC curves of (A) DVB15-BMA35 composite heated at 130°C for 4 h, (B) soy hulls, and (C) DVB15-BMA35 composite heated at 130°C for 5 h at 276 psi and postcured at 150°C for 2 h.

To fully cure the soybean oil-based resin during the composite processing, a longer cure sequence at higher temperatures was clearly required [see Fig. 1(A)]. For that reason, the cure time was increased to 5 h at 130°C and 276 psi. To ensure complete cure of the resin, a postcure of 2 h at 150°C and atmospheric pressure was tried. Figure 1(C) shows the DSC of a sample subjected to that cure sequence. In Figure 1(C), the peaks at 135 and 170°C have completely disappeared, indicating that the resin was completely cured after the longer heating sequence. Also, it is noticeable that the endothermic peak in Figure 1(C) is much less pronounced than in Figure 1(A,B). This peak is attributed to volatilization of compounds during thermal degradation of the hemicellulose.[28] This volatilization process occurs more easily in the absence of resin or in the presence of partially cured resin. The completely cured polymer network entraps soy hull particles, inhibiting volatilization. This particle entrapment is not as effective in the presence of the partially cured resin as the network is not fully formed and contains regions of lower molecular weight chains and lower crosslink density in the composite. Another reason for the lower endothermic peak in Figure 1(C) may be partial degradation of the hemicellulose during the longer cure process. A comparison of the DTA curves for the soy hulls (Fig. 2) and the DVB15-BMA35 composite (Fig. 3) also shows that degradation of hemicellulose starts at lower temperatures in the absence of the resin.

As a fully cured resin was desired for the preparation of composites in this work, all the samples prepared here were subjected to the same heat treatment: 5 h at 130°C and 276 psi, followed by a

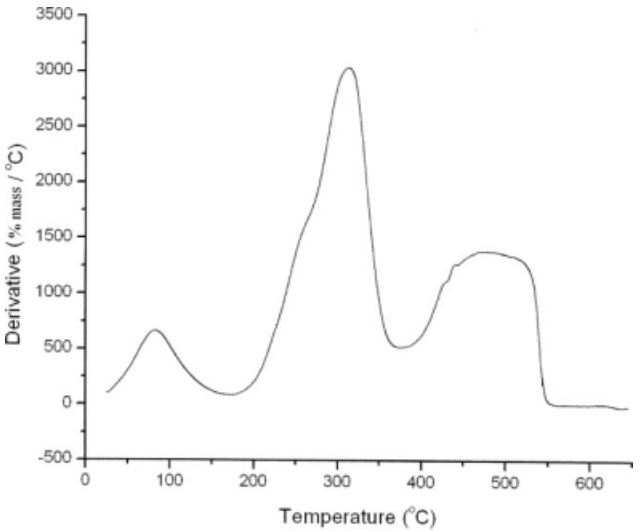

Figure 2 DTA curve of soy hulls.

postcure of 2 h at 150°C and atmospheric pressure (the pressure was different than 276 psi where indicated).

Dynamic mechanical analysis

From Table I, the effects of filler/resin ratio, particle size, and resin composition on the flexural properties of the composites can be obtained through analysis of the storage modulus (E') at 25°C. Table I also shows the glass transition temperatures (T_gs) of each sample as obtained from the tan δ curve by DMA.

The most distinctive characteristic of the composites prepared is the formation of a phase-separated matrix upon cure of the resin. The presence of two distinct T_gs in all samples is an evidence that compounds with different reactivity (such as CSO and DVB) have polymerized at different rates, producing a phase separation. For all samples, the first T_g (T_{g1}) occurred below −6°C, whereas the second T_g (T_{g2}) occurred above 57°C. The large difference between T_{g1} and T_{g2} indicates the formation of two phases with different properties and compositions. The phase associated with T_{g1} is believed to be a CSO-rich phase, composed mainly of less reactive species derived from CSO and DCPD. The phase associated with T_{g2} is probably a DVB-rich phase.

The reinforcing effect obtained when soy hulls are added to the resin can be clearly seen by comparing the values of T_{g2} for entry 1 and any other entry in Table I. For all reinforced samples (entries 2–18), T_{g2} occurs at a higher temperature than that of the unreinforced resin (entry 1, 57.3°C). The increase in T_{g2} ranges from 5% for entry 2 (60.2°C) to 46% for entry 13 (83.5°C). The effect is even more significant for the storage modulus, showing a minimum increase of 1.5 times in E' for entry 12 (234 MPa compared with 152 MPa for entry 1). The only property that does not seem to be significantly affected by the presence of reinforcement is T_{g1}. Indeed, T_{g1} is more sensitive to variations in the resin composition as will be explained later.

By increasing the pressure applied during cure from 92 to 368 psi (Table I, entries 2–5), a trend can be observed for E'. The storage modulus increases significantly from 298 MPa (entry 2) to 536 MPa (entry 4). When the applied pressure was 368 psi (entry 5), the storage modulus decreased to 356 MPa. The pressure during cure had a definite effect on the observed phase separation of the matrix as evidenced by the values of $T_{g2} - T_{g1}$ (Table I). As the pressure was increased from 92 to 276 psi, the difference in T_gs went from 84 to 107°C (entries 2–4, Table I), indicating an increase in the incompatibility of the two phases. Increasing the pressure to 368 psi showed no further effect on phase separation (entries 4 and 5, Table I). The relationship between cure pressure and phase separation is not fully understood at the present time and further tests are necessary to better explain these observations. One could argue that higher pressures force the resin to physically interact with the filler structure during cure (hence the increase in both T_gs, entries 2–4, Table I) and that this might favor stabilization of the CSO-rich phase through mixing with residual soybean oil from the soy hulls (see Table IV, entry 1), yielding an even lower polymerization rate for CSO and a greater phase separation. The influence of the residual oil from the filler on the T_g of the resin has been noted previously, where samples prepared with extracted filler showed higher T_gs than samples prepared with fillers containing residual oil.[25] In this work, the presence of fillers clearly contributes to phase separation of the resin, as noticed from the

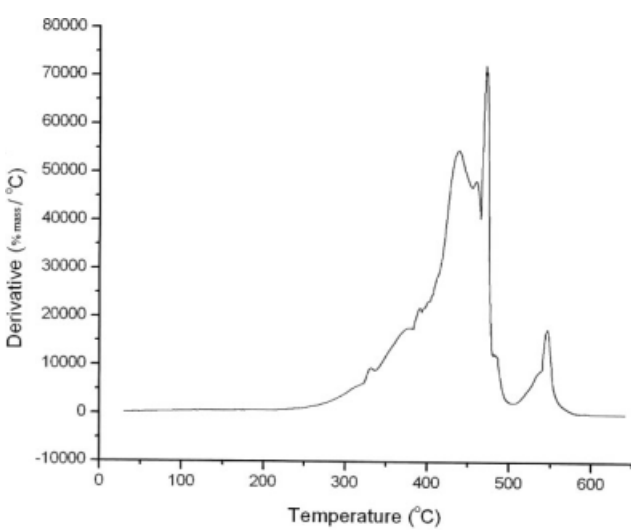

Figure 3 DTA curve of DVB15-BMA35 (filler/resin ratio = 50 : 50 and particle size <425 μm).

TABLE I
Glass Transition Temperatures (T_gs) and Storage Modulus (E') at 25°C of the Composites Prepared

Entry	Sample[a]	Filler/resin ratio (wt %)	Particle size (μm)	T_{g1} (°C)	T_{g2} (°C)	$T_{g2} - T_{g1}$ (°C)	E' at 25°C (MPa)
1	Resin[b]	–	–	−31	57	88	152
2	92 psi	50/50	<425	−24	60	84	298
3	184 psi	50/50	<425	−26	74	100	315
4	DVB15-BMA35	50/50	<425	−32	75	107	536
5	368 psi	50/50	<425	−31	76	107	356
6	DVB10-DCPD5-BMA35	50/50	<425	−12	68	80	492
7	DVB5-DCPD10-BMA35	50/50	<425	−8	73	81	340
8	DVB15-DCPD10-BMA25	50/50	<425	−14	74	88	686
9	DVB10-DCPD10-BMA30	50/50	<425	−18	69	87	291
10	DVB15-BMA35	60/40	<425	−32	76	108	416
11	DVB10-DCPD5-BMA35	60/40	<425	−17	75	92	318
12	DVB5-DCPD10-BMA35	60/40	<425	−7	65	72	234
13	DVB15-DCPD10-BMA25	60/40	<425	−13	84	97	384
14	DVB15-BMA35	60/40	<177	−36	74	110	456
15	DVB10-DCPD5-BMA35	60/40	<177	−12	72	84	326
16	DVB5-DCPD10-BMA35	60/40	<177	−13	73	86	262
17	DVB15-DCPD10-BMA25	60/40	<177	−29	79	108	411
18	DVB10-DCPD10-BMA30	60/40	<177	−32	65	97	333

[a] The cure was conducted at 276 psi unless otherwise noted.
[b] DVB15-BMA35 without filler.

$T_{g2} - T_{g1}$ values for entries 1, 4, 10, and 14 in Table I (88, 107, 108, and 110°C, respectively).

As seen from a comparison of entries 4, 6–8, and 10–13 in Table I, E' decreases considerably (at least 31% from entry 7 to 12) when a higher load of filler is used. Indeed, the higher filler content affects the dispersion and polymerization of the resin, yielding materials with increased flaws and/or weak points. The effect of filler/resin ratio on the T_gs is not clear, as most of the variations are negligible, except for the T_{g2} of entries 8 and 13 where there is a variation of 10°C.

The particle size of soy hulls has less effect in E' than the filler/resin ratio, with a maximum improvement of ~ 10% when smaller particles are used (compare entries 10 and 14 in Table I). Comparison of entries 10–13 and 14–17 in Table I reveals an overall improvement in storage modulus whenever smaller particles are used as the filler. At the same wt %, soy hulls having a smaller particle size present a higher density, accounting for a lower volume of material and a higher surface area when compared with larger particle sizes. The smaller particles allow better dispersion of the filler in the resin, enhancing the filler–resin interaction and consequently improving the composites' mechanical properties. Although some variations in T_gs can be observed when comparing entries 10–13 and 14–17 in Table I, they do not follow any particular trend that can be related to the properties of the final composites.

As expected from its structure and reactivity, DVB is the major structural comonomer in the resin; so E' is expected to drop whenever DVB is substituted by DCPD. As a matter of fact, this can be observed throughout Table I, and the most evident change is seen when comparing entries 14 and 16, where substitution of 10 wt % DVB by 10 wt % DCPD represents a loss of nearly 43% in E'. As far as the T_gs are concerned, a net increase in T_{g1} is observed when larger amounts of DCPD are present in the resin, whereas T_{g2} is not affected by the resin composition to the same extent (for example, entries 10–12). This suggests that DCPD is incorporated preferentially into the CSO-rich phase, increasing its crosslink density and augmenting T_{g1}. Another overall trend can be observed when comparing the values of $T_{g2} - T_{g1}$ for various resin compositions. As DVB is replaced by DCPD, a significantly lower difference in the two T_gs is obtained.

Tensile tests

The tensile test results for all composites prepared in this work are shown in Table II. From the results obtained, it can be seen that the tensile strength of the composites is lower for higher filler/resin ratios (Table II; entries 3, 5–7, and 9–12). A similar trend is observed for the Young's modulus, when these first two sets of results are compared, with the exception of entry 5. Although the variations in Young's modulus are proportionally less significant than those for the tensile strength, it is expected that high loads of filler affect the dispersion and polymerization of the resin, as mentioned earlier during the discussion of the DMA results. These observations are in agreement with previously published data.[25]

The effect of particle size was assessed by comparing the results summarized in entries 9–12 and 13–16

TABLE II
Young's Modulus and Tensile Strength of the Composites Prepared

Entry	Sample[a]	Filler/resin ratio (wt %)	Particle size (μm)	Young's modulus (MPa)	Tensile strength (MPa)
1	92 psi	50/50	<425	542 ± 27	2.4 ± 0.1
2	184 psi	50/50	<425	414 ± 18	1.4 ± 0.3
3	DVB15-BMA35	50/50	<425	672 ± 31	2.6 ± 0.2
4	368 psi	50/50	<425	551 ± 60	2.4 ± 0.1
5	DVB10-DCPD5-BMA35	50/50	<425	480 ± 58	1.8 ± 0.1
6	DVB5-DCPD10-BMA35	50/50	<425	473 ± 62	1.5 ± 0.2
7	DVB15-DCPD10-BMA25	50/50	<425	645 ± 74	2.3 ± 0.2
8	DVB10-DCPD10-BMA30	50/50	<425	441 ± 51	1.4 ± 0.2
9	DVB15-BMA35	60/40	<425	663 ± 59	2.0 ± 0.3
10	DVB10-DCPD5-BMA35	60/40	<425	636 ± 73	1.5 ± 0.2
11	DVB5-DCPD10-BMA35	60/40	<425	406 ± 46	0.7 ± 0.1
12	DVB15-DCPD10-BMA25	60/40	<425	569 ± 81	2.2 ± 0.1
13	DVB15-BMA35	60/40	<177	804 ± 63	2.5 ± 0.2
14	DVB10-DCPD5-BMA35	60/40	<177	468 ± 47	1.7 ± 0.3
15	DVB5-DCPD10-BMA35	60/40	<177	351 ± 50	0.9 ± 0.2
16	DVB15-DCPD10-BMA25	60/40	<177	641 ± 18	1.8 ± 0.3
17	DVB10-DCPD10-BMA30	60/40	<177	490 ± 79	1.3 ± 0.3

[a] The cure was conducted at 276 psi unless otherwise noted.

in Table II (samples having soy hull diameters <425 and <177 μm, respectively). The results show an improvement in tensile strength whenever smaller particles are used as the filler, except for the results reported in entry 16 of Table II. The overall trend observed here is in agreement with the observations made when discussing the DMA results. Similar effects were observed with spent germ biocomposites prepared from a tung oil resin.[25] For the Young's modulus, no regular trend was observed when comparing samples with different filler particle sizes.

Variations in the resin composition can affect significantly both the Young's modulus and the tensile strength of the composites, as can be seen when comparing entries 13 and 15 in Table II. For example, a difference of more than 50% in both properties is observed when 10 wt % DVB in the resin is substituted by 10 wt % DCPD. Indeed, because of the differences in reactivity and stability of the monomers, gradual substitution of 5 wt % of DVB by 5 wt % DCPD yields materials with lower tensile strength and Young's modulus (compare entries 3, 5, 6, 9–11, and 13–15 in Table II).

Substitution of BMA by DCPD has a lesser effect on the composites' properties than replacement of DVB by DCPD, as shown earlier. When 10 wt % of the comonomer BMA was replaced by 10 wt % DCPD (Table II, entries 7, 12, and 16 when compared with entries 3, 9, and 13), a drop in both the Young's modulus and the tensile strength was observed. The change is within the experimental error for the tensile strengths observed in entries 9 and 12 (2.0 and 2.2 MPa, respectively), but represents a decrease of up to 28% between entries 13 and 16 (2.5 and 1.8 MPa, respectively). The decrease in Young's modulus follows the same trend with up to a 20% decrease seen when comparing entries 13 and 16 (804 and 642 MPa, respectively). These results are closely related to the structure and reactivity of DCPD. The presence of two double bonds in this latter compound accounts for its role as a crosslinker in the same manner as DVB. For that reason, samples containing 25 wt % of DVB + DCPD show a high crosslink density that compensates for the low reactivity of DCPD toward free radical processes. When the amount of crosslinkers drops to 20 wt % by substituting 5 wt % of DVB by 5 wt % of BMA (entries 8 and 17 in Table II), a significant loss in tensile properties is observed. The Young's modulus decreases to 441 MPa (entry 8) and 490 MPa (entry 17) while the tensile strength drops to 1.4 and 1.3, respectively (entries 8 and 17) because of a lower crosslink density. Therefore, it can be concluded that DVB is the component that is primarily responsible for the tensile properties in the composites we have prepared.

Further investigation of the influence of the processing pressure on the final composites' properties is needed to explain the results observed. So far, no regular trend is evident for either the Young's modulus or the tensile strength when the pressure is increased from 92 to 368 psi (entries 1–4, Table II). The best results were obtained for the sample cured at 276 psi. The Young's modulus for that sample is 672 MPa and the tensile strength is 2.6 MPa (Table II, entry 3).

Thermogravimetric analysis

The thermal stability of the composites has been studied by TGA, and the results obtained are

TABLE III
Degradation Temperatures for the Composites

Entry	Sample[a]	Filler/resin ratio (wt %)	Particle size (μm)	T_{10} (°C)	T_{50} (°C)	T_{95} (°C)
1	Soy Hulls	–	<425	204	325	545
2	Resin[b]	–	–	344	436	585
3	92 psi	50/50	<425	278	384	624
4	184 psi	50/50	<425	274	375	594
5	DVB15-BMA35	50/50	<425	275	383	610
6	368 psi	50/50	<425	279	384	572
7	DVB10-DCPD5-BMA35	50/50	<425	265	357	624
8	DVB5-DCPD10-BMA35	50/50	<425	264	352	535
9	DVB15-DCPD10-BMA25	50/50	<425	271	383	642
10	DVB10-DCPD10-BMA30	50/50	<425	266	367	578
11	DVB15-BMA35	60/40	<425	276	381	567
12	DVB10-DCPD5-BMA35	60/40	<425	267	360	609
13	DVB5-DCPD10-BMA35	60/40	<425	269	365	623
14	DVB15-DCPD10-BMA25	60/40	<425	268	364	609
15	DVB15-BMA35	60/40	<177	266	378	551
16	DVB10-DCPD5-BMA35	60/40	<177	267	373	540
17	DVB5-DCPD10-BMA35	60/40	<177	255	355	588
18	DVB15-DCPD10-BMA25	60/40	<177	261	366	601
19	DVB10-DCPD10-BMA30	60/40	<177	266	379	590

[a] The cure was conducted at 276 psi unless otherwise noted.
[b] DVB15-BMA35 without filler.

presented in Table III. From the thermal degradation pattern of the composites, three temperatures are of particular interest: (1) the temperature at which 10 wt % of the sample has degraded (T_{10}), (2) the temperature at which 50 wt % of the sample has degraded (T_{50}), and (3) the temperature at which 95 wt % of the sample has degraded (T_{95}).

From entry 1 of Table III, it can be seen that initial degradation of the soy hulls starts near 200°C (T_{10} = 204°C) and the fibers are 95% degraded at 545°C (T_{95} = 545°C). For the unreinforced resin (Table III, entry 2), degradation starts near 344°C (T_{10} = 344°C) and is mostly finished at 586°C (T_{95} = 586°C). By reinforcing the resin with soy hulls, the thermal stability of the filler is significantly increased as the T_{10} values for all samples (entries 2–19) are higher than 255°C, representing an increase of at least 25%. This can be confirmed by analysis of the DTA curves of the soy hulls (Fig. 2) and the DVB15-BMA35 composite (Fig. 3). As seen in Figure 2, after the initial loss of water, the soy hulls start to degrade above 190°C, whereas the composite degradation only starts above 260°C. T_{50} is also improved in the presence of the resin, although a maximum increase of only 18% is seen (entries 5, 6, and 9). T_{95} seems to be affected in an irregular manner by the resin, so no conclusions can be drawn here.

Other parameters, such as pressure during cure, filler/resin ratio, particle size, and resin composition, seem to have no clear cut effect on the T_{10}, T_{50}, and T_{95} values. Indeed, T_{10} varies from 256°C (entry 17) to 279°C (entry 6), whereas T_{50} ranges from 352°C (entry 8) to 384°C (entry 3), and T_{95} goes from 535°C (entry 8) to 642°C (entry 9) without any regular pattern being evident.

Soxhlet extraction

The Soxhlet extraction results are presented in Table IV. Figure 4 shows the ^{1}H-NMR spectra of soybean oil (SOY), CSO and the extracts of soy hulls (SH), the pure resin and one of the composites prepared (DVB15-BMA35).

From the results in Table IV, it can be observed that the majority of the starting materials (82–92 wt %) get incorporated into the final composites, forming a material that is relatively insoluble in CH_2Cl_2. Soy hulls alone (Table IV, entry 1) yield 10 wt % of soluble materials, identified as being mainly soybean oil by ^{1}H-NMR spectroscopic analysis [Fig. 4(C)]. The unreinforced resin (entry 2) shows a total of 13 wt % of soluble materials after Soxhlet extraction. Characterization of the extract by ^{1}H-NMR spectroscopic analysis indicates CSO to be the major component and traces of BMA can be detected (peak at 4.05 ppm) [Fig. 4(D)].

The difference in pressure during the cure seems to have no effect on the percent soluble materials obtained from the composites (Table IV, entries 3–6). In fact, the 2 wt % difference observed between entries 6 and 3–5 is negligible. Also, the filler/resin ratio shows no significant effect on the percent soluble materials from the composites. Considering that the resin and the soy hulls are each responsible for 10–13 wt % of soluble materials, a higher filler/resin

TABLE IV
Extraction results

Entry	Sample[a]	Filler/resin ratio (wt %)	Particle size (μm)	% Soluble	% Insoluble
1	Soy Hulls	–	<425	10	90
2	Resin[b]	–	–	13	87
3	92 psi	50/50	<425	14	86
4	184 psi	50/50	<425	14	86
5	DVB15-BMA35	50/50	<425	14	86
6	368 psi	50/50	<425	12	88
7	DVB10-DCPD5-BMA35	50/50	<425	8	92
8	DVB5-DCPD10-BMA35	50/50	<425	10	90
9	DVB15-DCPD10-BMA25	50/50	<425	9	91
10	DVB10-DCPD10-BMA30	50/50	<425	11	89
11	DVB15-BMA35	60/40	<425	12	88
12	DVB10-DCPD5-BMA35	60/40	<425	9	91
13	DVB5-DCPD10-BMA35	60/40	<425	14	86
14	DVB15-DCPD10-BMA25	60/40	<425	9	91
15	DVB15-BMA35	60/40	<177	14	86
16	DVB10-DCPD5-BMA35	60/40	<177	15	85
17	DVB5-DCPD10-BMA35	60/40	<177	18	82
18	DVB15-DCPD10-BMA25	60/40	<177	15	85
19	DVB10-DCPD10-BMA30	60/40	<177	16	84

[a] The cure was conducted at 276 psi unless otherwise noted.
[b] DVB15-BMA35 without filler.

ratio was not expected to change the final amount of soluble materials in the composites. Indeed, a comparison of the percent soluble materials for similar resins with different filler/resin ratios (Table IV; entries 5, 7–9, and 11–14) shows a maximum difference of 4 wt % between entries 8 and 13 in Table IV.

Unlike the filler/resin ratio, the particle size does seem to affect the percentage of soluble materials in the final composites. A comparison of entries 11–14 and 15–18 in Table IV shows an average increase of 5 wt % in the amount of soluble materials when particles smaller than 177-μm diameter are used, instead

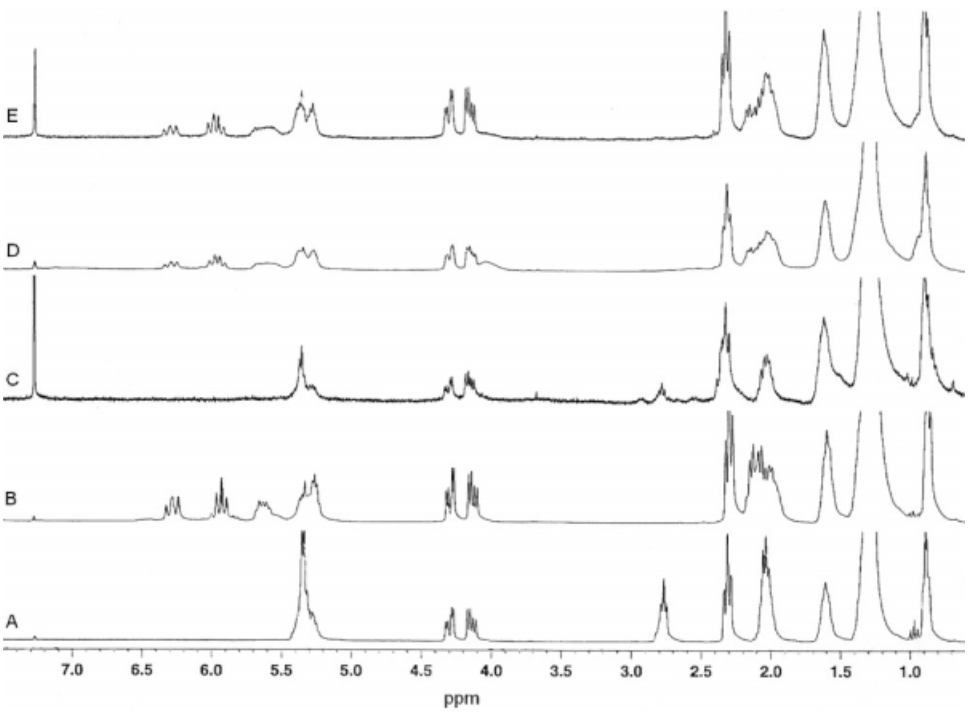

Figure 4 ^{1}H-NMR spectra of (A) soybean oil, (B) CSO, (C) soy hulls' extract, (D) unreinforced resin extract (composition: 50 wt % CSO, 35 wt % BMA, and 15 wt % DVB), and (E) composite extract (composition: resin = DVB15-BMA35, filler/resin ratio = 50/50, and particle size <425 μm). Spectrum E is representative of extracts from all composites.

of particles smaller than 425 μm diameter. With a higher surface area, smaller particles are expected to have a greater interaction with the resin. As proposed earlier when discussing the DMA results, the greater interaction between filler and resin may lead to mixture of the unreactive residual oil from the soy hulls with the CSO-based resin, which would decrease the overall reactivity of the matrix, yielding more soluble content. The reasons behind this observations are not yet fully clear and further studies are necessary to determine the origin of the observed behavior.

Finally, no particular pattern has been observed for the effect of resin composition on the amount of soluble material in the composites. It is assumed that all components are similarly incorporated into the matrix, with the exception of CSO. From a comparison of the ^{1}H-NMR spectra [Fig. 4(B,E)], the extract of the composites is believed to be primarily CSO, confirming our prediction that CSO is not likely to be fully incorporated because of its lower reactivity.

Scanning electron microscopy

Figure 5 shows the SEM images of cryofractured (A–D) and cut (E–H) surfaces of composite samples. Taking as the reference the sample shown in Figure 5(A,E), the images illustrate the effect of having the same resin composition and different cure pressures [Fig. 5(B,F)], filler/resin ratios [Fig. 5(C,G)], and filler particle sizes [Fig. 5(D,H)]. By analyzing the images, it is possible to better understand how some parameters change the filler–resin interaction and to correlate these effects with some of the properties obtained for the composites.

The cryofractured images [Fig. 5(A–D)] provide imortant information about the filler–resin interaction. From the absence of holes caused by fiber pullout or other similar events during fracture, it appears that there is a good interaction between the soy hulls and the matrix. The voids observed in the images are mainly the result of shrinkage during cure [Fig. 5(A–C)]. In Figure 5(D), the smaller soy hulls and their relatively good dispersion throughout the matrix make it difficult to distinguish between shrinkage cracks and structural voids in the sample.

In an attempt to evaluate the filler dispersion in the matrix, the composites were cut and the cross sections were observed by SEM [Fig. 5(E–H)]. The effect of pressure during cure can be assessed by the comparison of Figure 5(E,F). It can be seen that considerably fewer shrinkage cracks appear in the sample cured at 276 psi [Fig. 5(F)] than in the sample cured at 92 psi [Fig. 5(E)], yielding a more compact structure with less voids and more particles completely surrounded by the polymer matrix. This could explain the improvement in dynamic flexural properties for the sample cured at a higher pressure (Table I, entries 2 and 4). Improvements in tensile properties were also observed for these samples (Table II, entries 1 and 3); although a consistent explanation fails for the samples cured at 184 psi and 368 psi (Table I, entry 5, and Table II, entries 2 and 4).

A comparison of Figure 5(F,G) gives information about filler/resin ratio effects on the structure of the composites. The sample having a higher filler/resin ratio [Fig. 5(G)] exhibits considerably bigger flaws and voids than the sample with a 50 : 50 filler/resin ratio [Fig. 5(F)]. This is presumably caused by an absence of resin between the filler particles in some regions of the composite. This can explain the drop in storage modulus observed in Table I, entries 4, 6–8, and 10–13. For the tensile test, an overall decrease in E and in the tensile strength was observed (Table II, entries 3, 5–7, and 9–12), but again a consistent explanation fails when comparing the Young's modulus of entries 5 and 10 in Table II.

The most significant differences are observed when comparing particle size effects in the structure of the composites [Fig. 5(G,H)]. From the SEM images, it is clear that composites prepared with smaller particle sizes exhibit better dispersion of the soy hulls in the matrix. It is easily seen that the voids present in Figure 5(H) are much smaller than those in Figure 5(G), which may explain the better properties obtained for the former composite (Table I, entries 10 and 14, and Table II, entries 9 and 13). The higher contact surface between the soy hulls and the resin may account for the aforementioned effect on the percent soluble materials (Table IV, entries 11 and 15).

CONCLUSIONS

In this work, biocomposites have been prepared by the free radical polymerization of a CSO-based resin reinforced with soy hulls. An ideal cure sequence of 5 h at 130°C, followed by a postcure at 150°C for 2 h, has been established by a DSC study of the cure process. The effects of filler/resin ratio, particle size, and pressure during the cure process have been evaluated. It has been observed that the properties of the composites tend to decrease when higher filler/resin ratios or larger particle sizes are used. This behavior is closely related to impregnation of the filler by the resin; whenever good dispersion of the filler in the matrix is compromised, the mechanical properties of the composites are negatively affected. As the pressure applied during cure is increased up to 276 psi, an overall increase in the mechanical properties is detected by tensile test and DMA. The

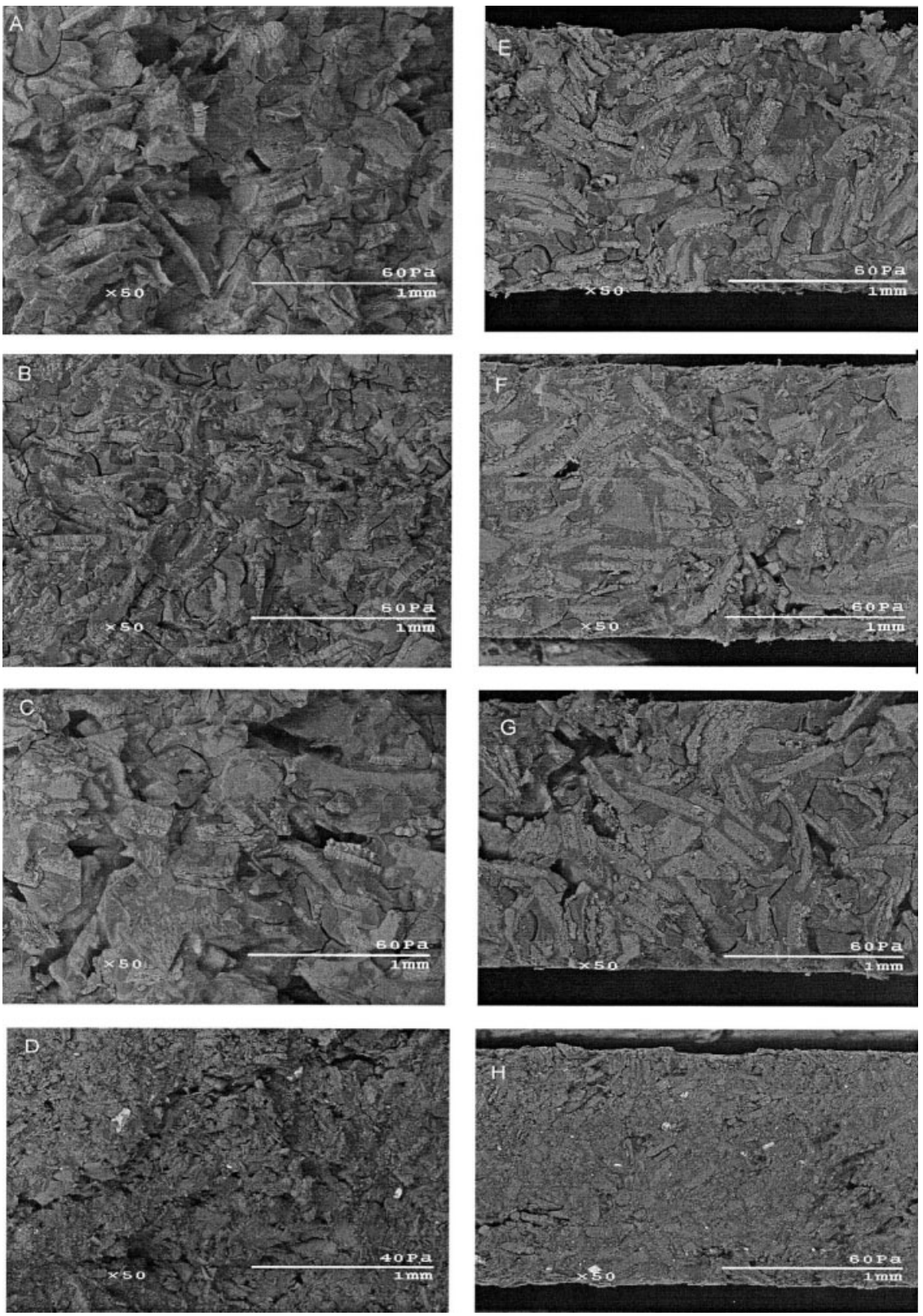

Figure 5 SEM images of (A) cryofractured DVB15-BMA35, 50 : 50 filler/resin ratio, particle size <425 μm, cured under 92 psi; (B) cryofractured DVB15-BMA35, 50 : 50 filler/resin ratio, particle size <425 μm, cured under 276 psi; (C) cryofractured DVB15-BMA35, 60 : 40 filler/resin ratio, particle size <425 μm, cured under 276 psi; (D) cryofractured DVB15-BMA35, 60 : 40 filler/resin ratio, particle size <177 μm, cured under 276 psi; (E) cut DVB15-BMA35, 50 : 50 filler/resin ratio, particle size <425 μm, cured under 92 psi; (F) cut DVB15-BMA35, 50 : 50 filler/resin ratio, particle size <425 μm, cured under 276 psi; (G) cut DVB15-BMA35, 60 : 40 filler/resin ratio, particle size <425 μm, cured under 276 psi; and (H) cut DVB15-BMA35, 60 : 40 filler/resin ratio, particle size <177 μm, cured under 276 psi.

properties decrease when a higher pressure (368 psi) is applied.

The matrix is identified as being phase separated, which is probably related to the difference in reactivity of CSO and the other monomers employed in the resin. Although good thermal stabilities and promising properties are obtained for the composites presented here, better results might be achieved by using more reactive oils, such as conjugated linseed oil.

In terms of resin composition, a significant dependence of the properties on the DVB content is observed. Replacement of DVB by DCPD affects considerably the properties because of the differences in the reactivity of these two compounds. A loss in reactivity of the resin upon substitution of BMA by DCPD is compensated by a higher crosslink density, but the final properties of the composites are still lower than those of the reference resin (DVB15-BMA35).

The authors thank West Central Co-Op. for the soy hulls, and Professor Michael Kessler from the Department of Material Sciences and Engineering and Dr. Richard Hall from the Department of Natural Resource Ecology and Management at Iowa State University for the use of their facilities.

References

1. Ma, F.; Hanna, M. A. Bioresour Technol 1999, 70, 1.
2. Wexler, H. Chem Rev 1964, 64, 591.
3. Sharma, V.; Kundu, P. P. Prog Polym Sci 2006, 31, 983.
4. Jin, F.; Park, S. Polym Int 2008, 57, 577.
5. Mosiewicki, M.; Aranguren, M. I.; Borrajo, J. J Appl Polym Sci 2005, 97, 825.
6. Miyagawa, H.; Mohanty, A. K.; Burgueno, R.; Drzal, L. T.; Misra, M. J Polym Sci Part B: Polym Phys 2007, 45, 698.
7. Li, F.; Larock, R. C. J Appl Polym Sci 2001, 80, 658.
8. Li, F.; Hasjim, J.; Larock, R. C. J Appl Polym Sci 2003, 90, 1830.
9. Andjelkovic, D. D.; Valverde, S. M.; Henna, P. H.; Li, F.; Larock, R. C. Polymer 2005, 46, 9674.
10. Andjelkovic, D. D.; Larock, R. C. Biomacromolecules 2006, 7, 927.
11. Li, F.; Larock, R. C. Biomacromolecules 2003, 4, 1018.
12. Kundu, P. P.; Larock, R. C. Biomacromolecules 2005, 6, 797.
13. Henna, P. H.; Andjelkovic, D. D.; Kundu, P. P.; Larock, R. C. J Appl Polym Sci 2007, 104, 979.
14. Valverde, M. S.; Andjelkovic, D. D.; Kundu, P. P.; Larock, R. C. J Appl Polym Sci 2008, 107, 423.
15. Lima, D. G.; Soares, V. C. D.; Ribeiro, E. B.; Carvalho, D. A.; Cardoso, E. C. V.; Rassi, F. C.; Mundim, K. C.; Rubim, J. C.; Suarez, P. A. Z. J Anal Appl Pyrolysis 2004, 71, 987.
16. Pakdeechanuan, P.; Intarapichet, K.; Fernando, L. N.; Grun, I. U. J Agric Food Chem 2005, 53, 923.
17. Mitchell, J. H.; Kraybill, H. R. J Am Chem Soc 1942, 64, 988.
18. Jung, M. O.; Yoon, S. H.; Jung, M. Y. J Agric Food Chem 2001, 49, 3010.
19. Jung, M. Y.; Ha, Y. L. J Agric Food Chem 1999, 47, 704.
20. Larock, R. C.; Dong, X.; Chung, S.; Reddy, C. K.; Ehlers, L. E. J Am Oil Chem Soc 2001, 78, 447.
21. Li, F.; Larock, R. C. J Appl Polym Sci 2000, 78, 1044.
22. Li, F.; Hanson, M. V.; Larock, R. C. Polymer 2001, 42, 1567.
23. Li., F.; Larock, R. C. J Polym Environ 2002, 10, 59.
24. Lu, Y.; Larock, R. C. Biomacromolecules 2006, 7, 2692.
25. Pfister, D. P.; Baker, J. R.; Henna, P. H.; Lu, Y.; Larock, R. C. J Appl Polym Sci 2008, 108, 3618.
26. Laszlo, J. A. J Agric Food Chem 1987, 35, 593.
27. Sessa, D. J. J Sci Food Agric 2004, 84, 75.
28. Yang, H.; Yan, R.; Chen, H.; Lee, D. H.; Zheng, C. Fuel 2007, 86, 1781.